J Mater Sci (2011) 46:3749–3752
DOI 10.1007/s10853-011-5288-z

Detector-grade CdZnTe:In crystals obtained by annealing

Pengfei Yu · Wanqi Jie · Tao Wang

Received: 5 December 2010 / Accepted: 13 January 2011 / Published online: 26 January 2011

Abstract A method for successfully obtaining detector-grade CdZnTe:In (CZT:In) crystals by annealing is described in this article. Pure Te is used as annealing source, which can provide sufficient deep-level Te antisites. Characterizations reveal that the resistivity is greatly enhanced by more than five orders after this annealing, thus the crystals can be use for radiation detectors. This is due to introduce efficient Te antisites to pin the Fermi level to the middle of the band gap. The EPD of dislocation reduces because the star-like Cd inclusions are eliminated by annealing. Investigation of annealing time shows that 240 h annealed CZT:In crystal with 7.8% energy resolution and 2.01×10^{-3} cm^2/V $\mu\tau$ value has the best detector performance.

Introduction

Cadmium zinc telluride (CZT) is an important wide band gap II–VI compound semiconductor, and widely used for X-ray fluorescence analysis, security inspection, medical imaging, and astronomy investigation due to its excellent opto-electrical properties [1–4]. Recently, In-doped CZT crystals have attracted much attention due to its high properties including large absorption coefficient, low bias voltage requirement, for the applications in the nuclear radiation detection and room temperature operation [5–7]. However, the quality of the material has not been completely optimized. In particular, defects related to Cd or Te inclusions have been recently shown to significantly affect the device performance [8, 9]. And inclusion phases inevitably exist in as-grown CZT crystals. Consequently, annealing is considered to be a very prospective way to solve this issue and potentially plays an important role in improving CZT quality.

Moreover, it is well known that in order to obtaining high resistivity, only the Fermi-level of material should be pinned at the mid band-gap position. Fiederle et al. [10] found that an important deep donor level with an energy level of about 0.75 eV below the conduction band was responsible for the high resistivity of CZT. This deep level can be assigned to tellurium antisite (Te_{Cd}). Based on this evidence, high-resistivity ($\rho > 10^{10}$ Ω cm) CZT:In crystals were grown with excess Te by Chu et al. [11]. The Fermi level is pinned to the deep-donor level of the doubly ionized Te antisites and the high resistivity is obtained through the compensation of V_{Cd} by Te_{Cd}. Inspired by this, it can be anticipated that as-grown low-resistivity CZT:In crystal will transform to high-resistivity one by annealing under Te atmosphere.

In this article, the authors report important results about detector-grade CZT:In crystals obtained by annealing low-resistivity ones under Te atmosphere for the first time. It suggests that the achievement of high resistivity for CZT material is due to the introduction of deep donor level Te_{Cd}.

Experimental

In this study, low-resistivity CZT:In wafers of about 2.5×10^5 Ω cm were chosen for annealing treatment. They

P. Yu (✉) · W. Jie · T. Wang
State Key Laboratory of Solidification Processing,
Northwestern Polytechnical University, Xi'an 710072, China
e-mail: ypfnwpu@gmail.com

P. Yu · W. Jie · T. Wang
School of Materials Science and Engineering,
Northwestern Polytechnical University, Xi'an 710072, China

were cut into slices in the size of $10 \times 10 \times 2$ mm^3 with the surface orientation of (111). Before annealing, all the slices were polished mechanically with MgO suspension and then etched with 5% bromine in methanol (Br_2–MeOH) for 2 min to remove the damaged surface layers. For annealing treatment, high-purity Te (7N) was sealed with CZT:In slices in the same quartz crucible under a vacuum of 10^{-5} Pa. Annealing experiments were carried out in a two-zone furnace. In order to reducing evaporation of Cd and Zn during the annealing process, the annealing temperature of both the slices and source was chosen as 773 K. Te vapor pressure can be calculated by the following equation [12]:

$$\lg p_{\mathrm{Te}} = (18.2 - 7525/T - 0.0004422T - 2.855\lg T)/760(\times 10^5\mathrm{Pa})(\mathrm{T} < 1261\mathrm{K}). \qquad (1)$$

The annealing time was 60, 120, and 24 h, respectively. In order to investigate dislocation of CZT:In crystal, both slices before and after annealing were etched by Everson solution [13] (HF/HNO_3/lactic acid = 1/4/25 mL).

IR transmission microscopy (Micronviewer 7290A, American Electrophysics Company) was used to detect inclusion phases. The electrical properties of the samples were measured at room temperature using an Agilent 4155C instrument. The energy resolution of the detector was measured with an ORTEC measurement system using a ^{241}Am γ-ray source at room temperature.

Results and discussion

The typical IR images of the CZT:In slices before and after annealing are given in Fig. 1. Figure 1a shows the micrograph of inclusions in as-grown wafer, where star-like inclusions (clear and blurry) can be observed. It is obvious that the inclusions are eliminated after annealing (Fig. 1b).Moreover, it is observed that the elimination of inclusions occurs when annealing time is more than 120 h. Brion et al. [14] observed six-pointed star-like inclusions in CdTe crystal grown with excess Cd by the Bridgman method, and EDX analysis indicated that the inclusion contained mainly Cd element. The growing condition of CZT crystal in this experiment is consistent with the condition of the crystal grown by Brion. Moreover, the authors have annealed the wafers under Cd atmosphere and the inclusions can not be eliminated completely, which is consistent with the result of Zhang et al. [15]. Therefore, the star-like inclusions are also Cd inclusions. The elimination of the inclusions may be explained that during annealing process, solid-state Cd inclusions are transformed to liquid Cd droplets because the annealing temperature is higher than the melting point of Cd (693 K). Then Cd droplets migrate to the surface of the wafers gradually like the thermomigration of Te [16]. Meanwhile, Te atoms diffuse into the bulk and react with Cd droplets, which also play an important role in the elimination of Cd inclusions via formation of Cd–Te in the bulk.

Figure 2 shows the typical etch pits of the CZT:In slices before and after annealing. The etch pit densities (EPD) of dislocation are counted in several regions, which are selected randomly on the slices. Their mean values are adopted in this analysis. For as-grown CZT:In crystal, the EPD of dislocation can be calculated to 2.6×10^5 cm^{-2}. After annealing, the EPD of dislocation are changed to 5.4×10^4, 1.2×10^4, and 7.6×10^4 cm^{-2} corresponding to 60, 120, and 240 h annealing, respectively. The reduction of dislocation can be ascribed to the elimination of Cd inclusions because dislocations often get together around inclusions. The reduction of the EPD value indicates a high crystalline quality. However, compared to 120 h annealed slice, the EPD value of 240 h annealed slice increases. This may be that the evaporation of Cd during longer annealing time (240 h) results in the production of dislocation.

The resistivity (ρ) is one of the most important properties for CZT radiation detectors [17]. The typical Current–voltage (I–V) measurement of annealed CZT:In slice is shown in

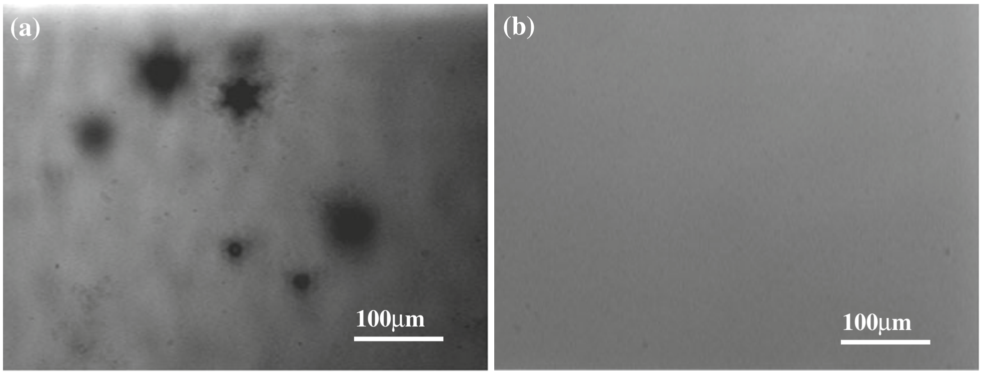

Fig. 1 IR images of the CZT:In wafers: **a** as-grown; **b** after annealing

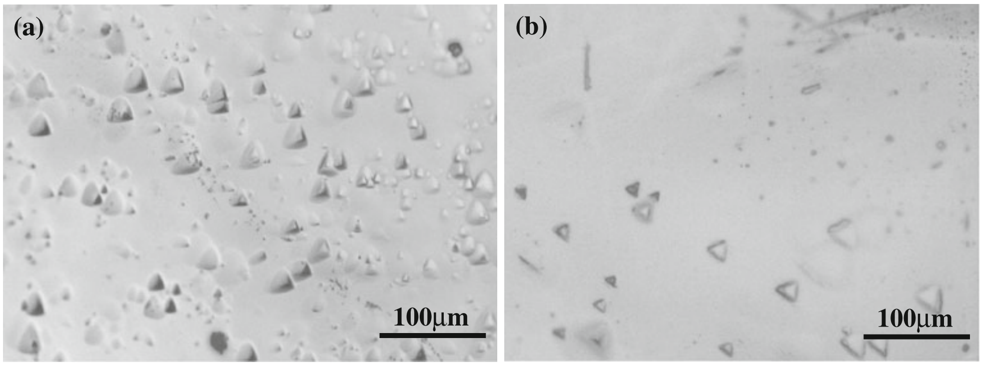

Fig. 2 Etch pits on (111) B-oriented CZT:In wafers after Everson etching: **a** as-grown; **b** after annealing

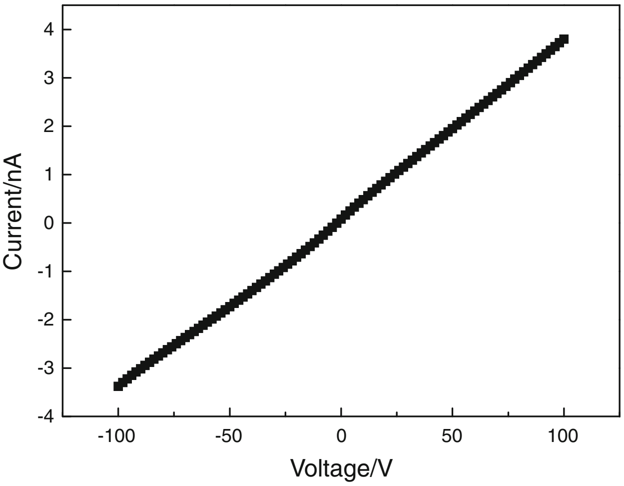

Fig. 3 The I–V curve of the annealed CZT wafer

Fig. 3, and it can be seen that the leakage current is lower than 4 nA. After annealing, the resistivity of 60, 120, and 240 h annealed CZT:In slices can reach the order of 10^9, 10^{10}, and 10^{11} Ω cm, respectively, which are much higher than that of as-grown CZT:In slice (2.5×10^5 Ω cm). High resistivity makes sure that the crystals can be used for radiation detectors. The improvement of resistivity suggests that the deep-donor level Te antisites are successfully introduced in CZT to pin the Fermi level at the mid band-gap position.

In fact, not all of indium atoms compensate Cd vacancy because of high indium concentration (about 5×10^{17} cm^{-2}) in as-grown CZT crystal, which is caused by self-compensation of indium. The self-compensation effect can be expressed by the following equation [18]:

$$\mathrm{In} + \mathrm{V}_{\mathrm{Cd}}^{2-} \leftrightarrow \mathrm{In}_{\mathrm{Cd}}^{+} + 3\mathrm{e}^{-}, \tag{2}$$

$$\mathrm{In}_{\mathrm{Cd}}^{+} + \mathrm{V}_{\mathrm{Cd}}^{2-} \leftrightarrow [\mathrm{In}_{\mathrm{Cd}}^{+}\mathrm{V}_{\mathrm{Cd}}^{2-}]^{-}, \tag{3}$$

$$\mathrm{In}_{\mathrm{Cd}}^{+} + [\mathrm{In}_{\mathrm{Cd}}^{+}\mathrm{V}_{\mathrm{Cd}}^{2-}]^{-} \leftrightarrow [2\mathrm{In}_{\mathrm{Cd}}^{+}\mathrm{V}_{\mathrm{Cd}}^{2-}]^{0}, \tag{4}$$

The self-compensation process reduces the doping efficiency of indium. Therefore, the as-grown CZT:In wafer has low resistivity. After annealing under Te atmosphere, $\mathrm{Te}_{\mathrm{Cd}}$ compensates the residual-Cd vacancies to form the neutral defect complex $[\mathrm{Te}_{\mathrm{Cd}}^{4+}\mathrm{V}_{\mathrm{Cd}}^{2-}]^{0}$. This can be expressed as follows,

$$\mathrm{Te}_{\mathrm{Cd}}^{4+} + 2\mathrm{V}_{\mathrm{Cd}}^{2-} \leftrightarrow [\mathrm{Te}_{\mathrm{Cd}}^{4+}2\mathrm{V}_{\mathrm{Cd}}^{2-}]^{0} \tag{5}$$

Te antisites are actually Te atoms located at Cd vacancies. In annealing process, Te atoms diffuse to the bulk and occupy some of the vacancy sites. Then Te-antisite and Cd-vacancy complexes form and the doubly ionized Te antisites pin the Fermi level at the mid band-gap position. Thus, the resistivity of CZT:In is improved so much.

Figure 4 shows ^{241}Am γ-ray spectra of the detectors fabricated with annealed CZT:In slices, passivated with $\mathrm{H_2O_2}$ solution after planar-electrode prepared on both two sides of the detectors. The bias voltage is 420 V, the shaping time is 1 μs. From Fig. 4, the energy resolution of the detectors fabricated by 60, 120, and 240 annealed CZT:In slices can be calculated to be 28.9, 11.1 and 7.8%,

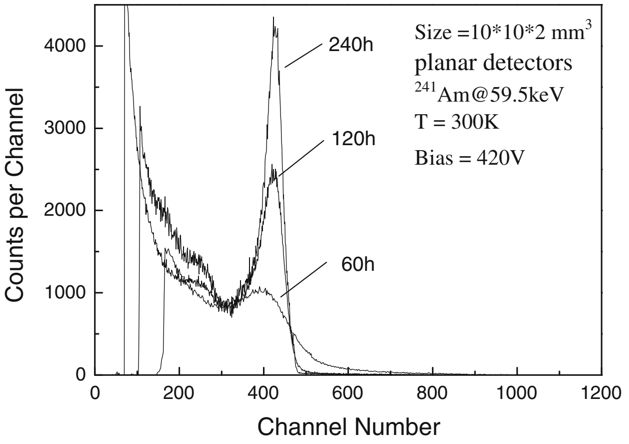

Fig. 4 ^{241}Am γ-ray energy spectra of CZT:In detectors with a planar structure

respectively. The mobility-lifetime products ($\mu\tau$) for electrons can be determined by Hecht equation [19]:

$$Q = Q_0 \times \frac{\mu\tau E}{d}\left[1 - \exp\left(\frac{-d}{\mu\tau E}\right)\right] \quad (6)$$

Q is the charge collection, Q_0 is the maximum collectible charge, $\mu\tau$ is the mobility-lifetime product, E is the applied electric field, and d is the thickness of the sample. Therefore, corresponding $\mu\tau$ values of CZT:In detectors are 7.28×10^{-4}, 1.66×10^{-3}, and 2.01×10^{-3} cm^2/V, respectively. 240 h annealed CZT:In slice has the best detector performance, which suggests that this slice has sufficient deep-level Te antisites to pin the Fermi level to the middle of the band-gap and has a minimal amount of carrier traps. It is an essential upgrade that the useless sample with low performance becomes the useful one for radiation detector.

Conclusions

In order to obtain detector-grade CZT:In crystals, low-resistivity CZT:In crystals were annealed under Te atmosphere. After annealing between 60 and 240 h, the EPD of dislocation reduced and the crystalline quality improved. The star-like Cd inclusions can be completely eliminated after more than 120 h annealing. The resistivity of the annealed CZT:In crystals was greatly enhanced due to introduce efficient deep-level Te antisites to pin the Fermi level to the mid band-gap position, which made the crystals could be used for radiation detectors. 240 h annealed CZT:In crystal with 7.8% energy resolution and 2.01×10^{-3} cm^2/V $\mu\tau$ value had the best detector performance.

Acknowledgements This study was supported by the National Natural Science Foundations of China under Grant nos. 50872111 and 50902114, and also supported by the 111 Project (B08040).

References

1. Eisen Y, Shor A (1998) J Cryst Growth 184/185:1302
2. Fiederle M, Feltgen T, Meinhardt J, Rogalla M, Benz KW (1999) J Cryst Growth 197:635
3. Li Q, Jie WQ, Fu L, Yang G, Bai XX, Zha GQ (2006) J Cryst Growth 295:124
4. Limousin O (2003) Nucl Instrum Meth Phys A 24:504
5. Lachish U (2001) J Cryst Growth 225:114
6. Yang G, Jie WQ, Li Q, Wang T, Li GQ, Hua H (2005) J Cryst Growth 283:431
7. Koley G, Liu J, Mandal KC (2007) Appl Phys Lett 90:102121
8. Bolotnikov AE, Camarda GS, Carini GA, Fiederle M, Li L, McGregor DS (2006) IEEE Trans Nucl Sci 53:607
9. Kim KH, Gul R, Carceln V, Bolotinkov AE, Carmarda GS, Yang G (2010) J Cryst Growth 312:781
10. Fiederle M, Eiche C, Salk M, Schwarz R, Benz KW (1998) J Appl Phys 84:6692
11. Chu M, Terterian S, Ting D (2004) IEEE Trans Nucl Sci 51:2408
12. Zhang B, Sang WB, Li WW, Ming JH (2004) J Semicond 25:1148
13. Everson WJ, Ard CK, Sepich JL, Dean BE, Neugebauer GT (1995) J Electron Mater 24:506
14. Brion HG, Mewes C, Hahn I, Schäufele U (1993) J Cryst Growth 134:282
15. Zhang XW, Zhao ZL, Zhang PJ, Ji RB, Li QB (2009) J Cryst Growth 311:288
16. Rudolph P, Engel A, Schentke I, Grochocki A (1995) J Cryst Growth 147:303
17. Yu PF, Jie WQ, Wang T (2010) J Cryst Growth 312:2879
18. Wang T, Jie WQ, Zeng DM, Yang G, Xu YD, Liu WH, Zhang JJ (2008) J Mater Res 23:1389
19. Jones KA, Ciampi G, Skrip CE, Lynn KG (2007) Proc SPIE 6706:670607